Cool pulsed molecular microbeam

Bum Suk Zhao, Marta Castillejo, Doo Soo Chung, Bretislav Friedrich, and Dudley Herschbach

Citation: Review of Scientific Instruments **75**, 146 (2004); doi: 10.1063/1.1630836

View online: http://dx.doi.org/10.1063/1.1630836

View Table of Contents: http://scitation.aip.org/content/aip/journal/rsi/75/1?ver=pdfcov

Published by the AIP Publishing

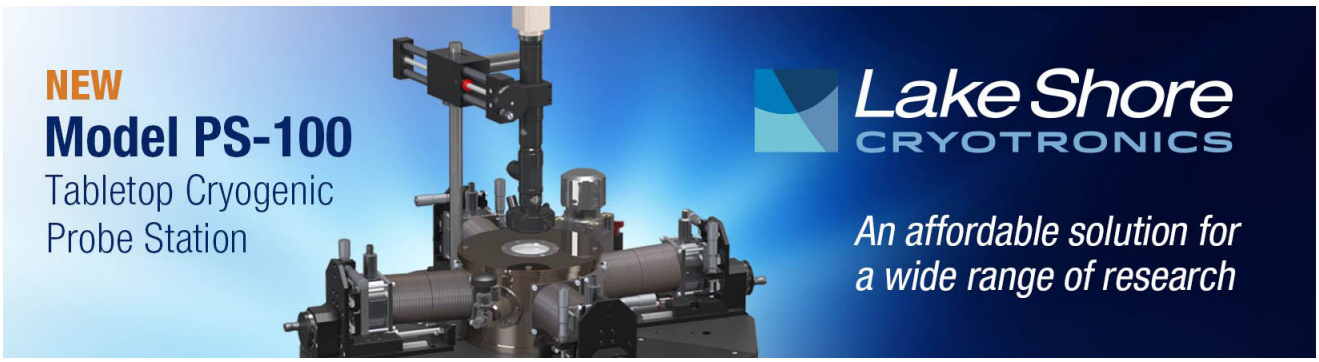

Cool pulsed molecular microbeam

Bum Suk Zhao,[a] Marta Castillejo,[b] Doo Soo Chung,[a] Bretislav Friedrich,[c] and Dudley Herschbach
Department of Chemistry and Chemical Biology, Harvard University, Cambridge, Massachusetts 02138

(Received 30 July 2003; accepted 21 September 2003)

We produce a cool pulsed supersonic molecular beam of CaF radicals essentially without recourse to pumping. The radicals are generated by laser ablating a solid precursor target in a small ablation cell of volume of about 0.01 cm^3. The target is ablated through a 750 μm orifice by a pulsed Nd:YAG laser. The ablation plume supersonically expands into a vacuum chamber and cools the initially hot CaF molecules seeded in it. We enhance the supersonic character of the expansion by feeding into the ablation cell about 10 Torr of He, Ar, or Xe carrier gas. The CaF molecules are probed by time-dependent laser absorption spectroscopy. With a Xe carrier, about 10^{12} CaF molecules are found to be seeded in a single pulse and cooled down to a terminal translational temperature of about 140 K. We expect that a wide variety of species, including highly unstable ones, will be amenable to forming such a cool intense molecular microbeam, to the benefit of spectroscopy, reaction dynamics, and microfabrication. © *2004 American Institute of Physics.*
[DOI: 10.1063/1.1630836]

I. INTRODUCTION

The scope of molecular collision and spectroscopic experiments has been greatly extended by means of molecular beam sources employing supersonic gas flow,[1,2] often in combination with pulsed nozzles,[3] or with laser-induced ablation to enable refractory species to be entrained in a gas flow.[4] This article describes a versatile source, employing supersonic flow, pulsing, and ablation in a way that minimizes size and pumping requirements. The key strategic features are to produce an ablation plume by directing a laser pulse through the exit orifice of the source, so that the plume is cooled as it undergoes a supersonic expansion while emerging from the orifice accompanied by a modest flow of carrier gas. The source, operated with 10 Torr of Xe as carrier, produces about 10^{12} of CaF radicals per pulse with a terminal translational temperature of about 140 K, an order of magnitude lower than that estimated for the initial ablation plume.

The chief motivation for development of this source came from work with a device designed to produce molecular beams with very low kinetic energy[5] and thereby enhance means to influence molecular trajectories by interaction with external fields, particularly required to achieve spatial trapping. The device employs a supersonic nozzle mounted near the tip of a hollow high-speed rotor, into which a permanent gas is fed continuously. Spinning the rotor with peripheral velocities of several hundred m/s, contrary to the direction of gas flow from the nozzle, markedly reduces the velocity in the laboratory frame of the emerging molecular beam. However, the continuous gas flow is a major limitation. It gives rise to a 360° spray that requires drastic pumping, as slow molecules are strongly scattered by background gas. To avoid this requires a means to pulse the source, synchronously with the rotor, so that the molecular beam is emitted only in the ''firing position.'' The ablation source described here, pulsed by a laser, is small enough to mount on a high-speed rotor and requires minimal pumping. These virtues, as well as the efficacy of cooling the ablation plume, indicate the source will prove useful in many other circumstances.

The CaF radical was chosen for initial tests as it is readily generated by ablation of CaF_2, can be conveniently monitored by laser absorption spectroscopy,[6] and is a candidate for magnetic trapping studies [akin to that done with CaH (Ref. 7)]. After describing the experimental apparatus, procedures, and results, we employ a simple gas-kinetic model[8] to estimate the terminal translational temperatures and the yield per pulse obtained for the CaF beam and find good agreement with results derived from laser absorption spectroscopy.

II. EXPERIMENTAL RESULTS

Our apparatus consists of a small ablation cell housed in a vacuum chamber. Figure 1 shows the cell and vacuum chamber along with the ablation and probe laser paths. The ablation cell, shown in greater detail in the inset, is made from a $\frac{1}{4}$ in. (6.35 mm) outer diameter copper rod 1.3 cm long, drilled to an inner diameter of 5 mm from one end and terminated by a 1 mm thick partition on the other. An orifice of 0.75 mm diam drilled through the partition along the cylindrical axis of the rod serves as a supersonic nozzle. The ablation cell is held by a swagelock feedthrough mounted on a Conftat flange and connected on the outside to a gas fill line equipped with a needle valve. The ablation cell houses a lump of a CaF_2 precursor target, affixed about 0.5 mm upstream from the orifice. The vacuum chamber, constructed

[a]Present address: School of Chemistry, Seoul National University, Seoul 151-747, Korea.
[b]Permanent address: Instituto de Química Física Rocasolano, CSIC Serrano 119, 28006 Madrid, Spain.
[c]Electronic mail: brich@jsbach.harvard.edu

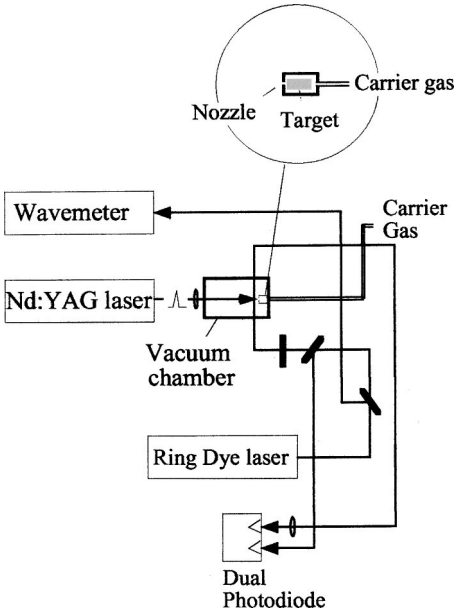

FIG. 1. Schematic view of the apparatus.

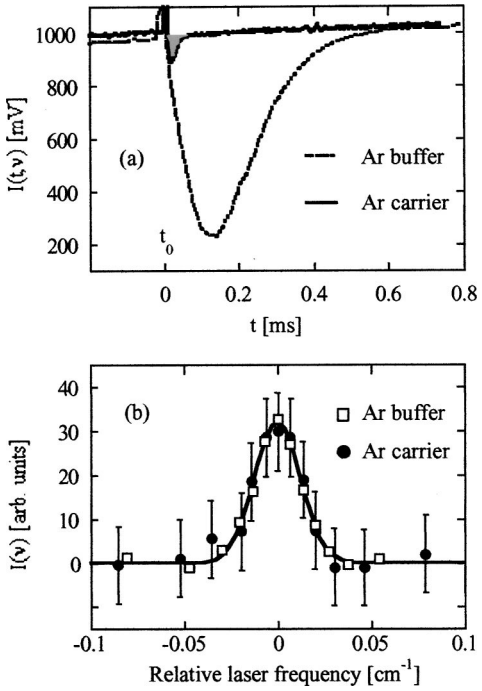

FIG. 2. (a) CaF on-resonance probe-laser signal (absorption time profile), $I(t,\nu=\nu_0)$, with (dashed line) and without (full line) buffer gas. The time zero (t_0) is defined by the time the Nd:YAG pulse is fired. (b) Integrated absorption signal, $I(\nu)$, in the presence (squares) and absence (circles) of buffer gas. The Doppler line fit (full line) corresponds to a temperature of 306 K, see the text. In the absence of buffer gas, about 10 Torr of Ar carrier gas is fed into the ablation cell. The $R_1(J''=11.5)$ transition within the $A^2\Pi(v'=0)\leftarrow X^2\Sigma(v''=0)$ band near 606 nm was used.

from standard stainless steel 2 $\frac{3}{4}$ in. Conflat-type vacuum hardware has three-way optical access through windows made of BK7, and is pumped by a small turbomolecular pump (not shown) at an effective pumping speed of about 10 l/s.

The target is ablated by a Nd:YAG pulsed laser, with a pulse duration of 5 ns and a typical energy of 10 mJ per pulse focused to a waist of about 200 μm, yielding an intensity of about 10^{10} W/cm^2. The target (made by Sophisticated Alloys) was vacuum hot pressed, which ensures a steady yield over about 10^{5-6} ablation pulses aimed at the same spot. We found the yield to be consistent from spot to spot.

The CaF molecules released into the gas phase by the ablation pulse are probed by laser absorption spectroscopy in the $A^2\Pi(v'=0)\leftarrow X^2\Sigma(v''=0)$ band near 606 nm.[9] Several rotational lines were probed in our experiments but all the data presented here pertain to the $R_1(J''=11.5)$ transition at 16 506.34 cm^{-1}.

The probe beam is produced by an actively stabilized ring dye laser (Coherent 699-21), operated with the Rhodamine 6G dye. The probe beam of 3.5 mm diam and typical power of 0.3 mW passes horizontally through the vacuum chamber next to the ablation cell orifice. This geometry gives the best sensitivity, of about 10^{-3}. The probe beam intensity is monitored by a balance photodiode detector (New Focus), whose reference input is fed with a fraction of the probe beam split before its entry into the vacuum chamber. The detector output is transduced to a digitizing oscilloscope (Tektronix) interfaced with a computer. The oscilloscope is triggered by the Q-switch control of the Nd:YAG laser and records the time profile of the detector signal output. The ablation pulse creates an intense white plasma glow. In order to avoid inundating the detector with the plume glow, we protect it with a bandpass interference filter; in addition, we keep the detector about 3 m away from the ablation cell to achieve spatial filtering. Despite these precautions, the glow remained more than noticeable (see below).

The time profiles were surveyed over a range of about 20 cm^{-1} at 16 500 cm^{-1}. Near a resonance, the time profiles were measured in steps of about 0.01 cm^{-1} over a range of about 0.2 cm^{-1}. The probe-laser frequency was measured with a wavemeter (Burleigh W-20) and the lines were assigned with the help of Ref. 9.

In order to facilitate finding the absorption signal due to ablated CaF molecules, we first carried out an auxiliary experiment. In this experiment, we filled the vacuum chamber with about 1 Torr of Ar gas. As demonstrated previously by the deCarvalho *et al.*,[10] the Ar gas serves as a buffer which thermalizes the ablated molecules via elastic collisions. Figure 2 displays typical results. Panel (a) shows the CaF time profiles $I(t,\nu)$ at the probe laser frequency $\nu=\nu_0$ corresponding to resonance for the $R_1(J''=11.5)$ transition. The dashed trace in Fig. 2(a) pertains to the CaF time profile with the buffer gas present. The time profile $I(t,\nu_0)$ exhibits a spike at the time the Nd:YAG laser is fired (this defines the time zero, t_0). The spike is due to the residual glow from the plume that reaches the detector. The detector signal then sharply drops, reaches a minimum at about 0.15 ms, and subsequently tapers off at about 0.7 ms after the ablation pulse. The drop in the signal is due to absorption, which is proportional, at a given time t and probe laser frequency ν, to the number of CaF($X^2\Sigma, v''=0, J''=11.5$) molecules present in the probed volume. The integral over the time profile, $\int|I(t,\nu)|dt\equiv I(\nu)$, is proportional to the total num-

ber of molecules generated by a single ablation pulse. The squares in Fig. 2(b) show the dependence of the integrated absorption signal $I(\nu)$ on the probe laser frequency (i.e., the line shape) for the $R_1(J''=11.5)$ transition. A Doppler line profile fitted to the data is shown in Fig. 2(b). It corresponds to a temperature of 306 ± 15 K, i.e., the temperature of the cell. Thus, we can conclude that the CaF molecules are fully thermalized by the buffer gas. Indeed, this is what we expect. In the course of the thermalization, the CaF molecules travel a distance $\Lambda_K \approx K^{1/2}/(n_{\mathrm{Ar}}\sigma)$, where n_{Ar} is the number density of the Ar buffer gas, σ is the elastic CaF–Ar cross section, and K is the number of elastic collisions. For $n_{\mathrm{Ar}} \approx 10^{16}$ cm^{-3} and taking $\sigma \approx 100$ Å^2 and $K=100$, we obtain $\Lambda_{100} \approx 1$ mm, i.e., well within the probed region centered about 2 mm downstream from the ablation cell orifice.

As we reduce the pressure of Ar in the vacuum chamber, the thermalization becomes less effective and ceases completely below about 100 mTorr, as the mean-free path of CaF in Ar then exceeds the dimensions of the probe region or the vacuum chamber itself. Figure 2(a) shows the $I(t,\nu_0)$ time profile (full curve) and Fig. 2(b) the absorption line shape (circles) of CaF seeded in about 15 Torr of Ar gas at a pressure in the vacuum chamber of about 10 mTorr, i.e., effectively in the absence of buffer gas. One can see that the time profile exhibits a spike at t_0 similar to the one in the time profile obtained in the presence of the buffer gas; again, the spike is due to the residual glow of the ablation plume. However, the time evolution of the absorption signal at later times looks quite different. Whereas in the presence of the buffer gas the time profile reflects the diffusion kinetics of CaF, in its absence the time profile reveals the time-of-flight distribution of CaF molecules in the pulsed molecular beam. The short flight time (i.e., high-velocity) tail of the distribution is, unfortunately, distorted by the plume glow. Nevertheless, the long-flight time (i.e., low-velocity) tail is not affected by the glow and so can be used to determine the lower limit of the CaF velocity. In order to extract the total absorption signal at a given probe laser frequency, $I(\nu)$, we integrate over the fraction of the time profile that corresponds to absorption. This fraction is indicated by the gray area in Fig. 2(a). The shape of the $R_1(J''=11.5)$ absorption line, shown by the squares in Fig. 2(b), was determined by integrating over such fractions of the absorption profiles measured at different probe laser frequencies. The Doppler line shape fitted to it happens to coincide with the one obtained with the buffer gas present, and yields a temperature of 306 ± 50 K. We have to appreciate that this terminal temperature is a result of considerable cooling, since the initial CaF temperature may be on the order of 10^3 K (see below). The increased uncertainty is due to the relatively large distortion of the absorption time profiles by the plume glow.

Figure 3 shows absorption time profiles of CaF obtained with different carriers. This set of data was corrected for the effect of the plume glow by subtracting the on-resonance time profile, $I(t,\nu_0)$, from a time profile that was measured with the probe laser tuned out of resonance, $I(t,\nu\neq\nu_0)$, i.e., we plot the quantity $I_c(t,\nu_0)=I(t,\nu\neq\nu_0)-I(t,\nu_0)$. Although the short-time portion of the profile is still somewhat obscured by the effects due to the plume light, we were able

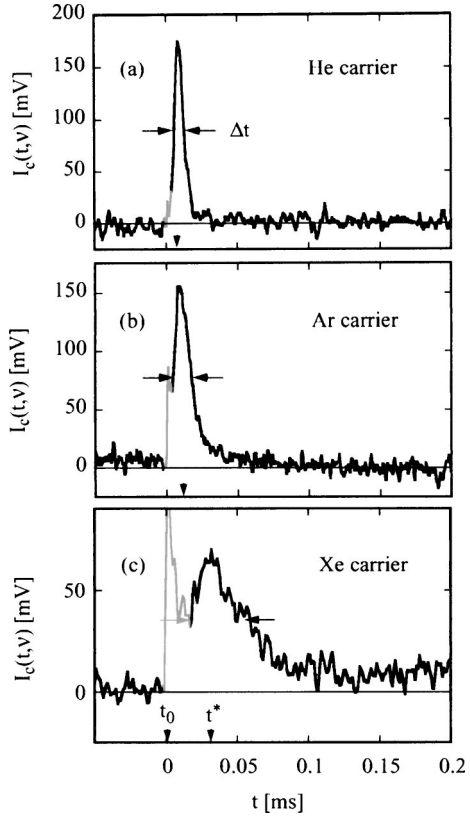

FIG. 3. Absorption time profiles, $I_c(t,\nu_0)$, of CaF obtained with different carriers. This set of data was corrected for the effect of the plume glow by subtracting the on-resonance time profile from an off-resonance profile, see the text. Here, Δt is the full width at half maximum of a time profile, t^* is the peak position of a time profile, and t_0 is the time when the ablation laser is fired. The $R_1(J''=11.5)$ transition within the $A^2\Pi(v'=0)\leftarrow X^2\Sigma(v''=0)$ band near 606 nm was used. See, also, Table I.

to recover most of the shape of the time-of-flight distributions of the CaF molecules. As shown in Table I, the peak positions of these distributions indicate that the CaF molecules are slowed down substantially in Xe compared with He, with the widths of the distributions, Δt, increasing correspondingly. Figure 4 shows the integrated absorption signal $I(\nu)$ for the $R_1(J''=11.5)$ transition as a function of the probe laser frequency obtained for different carrier gases. The full lines in each of the panels are Gaussian fits. From these we were able to extract the terminal temperature of the seeded CaF molecules, indicated in Table I. Thus, we see that the temperature variation of CaF in the different carrier gases

TABLE I. Characteristic parameters of the pulsed molecular microbeam of CaF in different carrier gases. Here, Δt is the full width at half maximum of the time profile, $\Delta\tau=\Delta t v/s$ is the full width at half maximum of the reduced time profile, t^* is the peak position of the time profile, and $\tau^*=t^*v/s$ is the peak position of the reduced time profile, see the text.

Carrier	Terminal temperature, T (K)	Δt (ms)	$\Delta\tau$	t^* (ms)	τ^*
He	740 ± 50	0.008 ± 0.005	4 ± 3	0.008 ± 0.005	4 ± 2
Ar	306 ± 50	0.014 ± 0.005	6 ± 3	0.01 ± 0.008	4 ± 2
Xe	136 ± 50	0.036 ± 0.01	10 ± 4	0.03 ± 0.01	8 ± 4

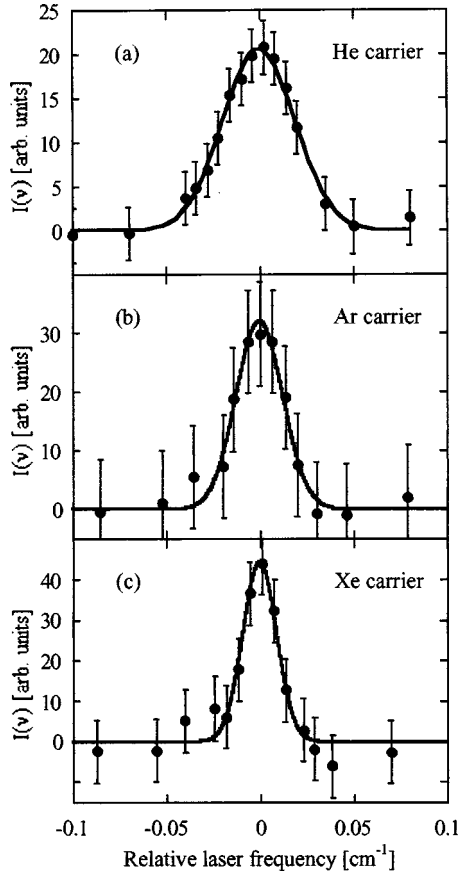

FIG. 4. Integrated absorption signal, $I(\nu)$, in the absence of buffer gas for different carriers. The $R_1(J''=11.5)$ transition within the $A^2\Pi(v'=0) \leftarrow X^2\Sigma(v''=0)$ band near 606 nm was used. The frequency scale is centered at 16 506.34 cm^{-1}. See the text.

exhibits trends consistent with those revealed by the time profiles.

III. DISCUSSION

In order to establish the correspondence between the time profiles and line shapes semiquantitatively, we sought to rescale the time profiles in the different carrier gases such that, apart from an intensity factor, these would coincide with one another. To this end, we redefined the time scale in terms of a time unit, t_n, yielding a reduced time $\tau = t/t_n$, independent of the carrier gas. For the time unit we chose the ratio of the flight path s of the CaF molecules ($s \approx 2$ mm) to their most probable velocity, v, i.e., $t_n = s/v$. The most probable terminal velocity of the CaF molecules in a given carrier can be approximated by[8]

$$v = \tfrac{1}{2}[u + (u^2 + 8kT/m_S)^{1/2}], \tag{1}$$

with T the terminal temperature of CaF, m_S the CaF mass, and

$$u = u_\infty (1 - T/T_0)^{1/2}, \tag{2}$$

the CaF flow velocity. In the last expression, T_0 is the stagnation temperature (i.e., assumed to be the common temperature of the seeded species and the carrier gas) and u_∞ is given by

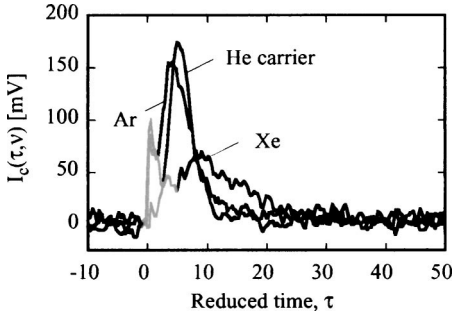

FIG. 5. Rescaled absorption time profiles, $I_c(\tau, \nu_0)$, of Fig. 3. The reduced time τ (abscissa) measures the flight time t in units of s/v, with s the distance between the nozzle orifice and the probe region, and v the most probable velocity of the CaF molecules in a given carrier gas. See, also, Table I and the text.

$$u_\infty = \left(\frac{2\bar{\gamma} k T_0}{(\bar{\gamma} - 1)\bar{m}} \right)^{1/2}, \tag{3}$$

where $\bar{\gamma} = f\gamma_S + (1-f)\gamma_C$ and $\bar{m} = f m_S + (1-f) m_C$ are the average Poisson coefficient and the average mass of the binary mixture, with f the fraction of the seeded species in the mixture, and γ_S, γ_C and m_S, m_C the Poisson coeffcients and the masses of the seeded species and of the carrier gas.

Given an effective stagnation volume of about 0.01 cm^3 and a Nd:YAG pulse energy of 10 mJ, we estimate that the stagnation temperature of the source can rise up to about 1500 K. Based on the absorbance and the measured pressure, P_C, of the carrier gas, we estimate that the fraction of CaF in the binary mixture is on the order of 1%. Figure 5 shows the rescaled time profiles in the different carrier gases for $T_0 = 1000$ K and $f = 0.01$. One can see that these pretty much fall in place. The reduced peak position of the time profile comes out close to $5t_n$.

The probed number density of the CaF molecules is approximately given by[8]

$$n \approx \frac{f n_C A}{16\pi L^2}, \tag{4}$$

where A the orifice surface area, L is the distance between the orifice and the probe laser beam path, and $n_C = P_C/(kT_0)$, with P_C the stagnation pressure of the carrier gas. For $L = 0.2$ cm, $f = 0.01$, $T_0 = 1000$ K, $P_C = 10$ Torr, and $A = \pi(d/2)^2$, we obtain $n \approx 10^{12}$ CaF molecules per cm^3. Given that the probed volume is about 1 cm^3, we estimate that about 10^{12} CaF molecules are formed. This is consistent with the observed absorption. The total number of molecules that contribute towards an absorption profile is given by

$$N(\nu) \approx \frac{bL}{\sigma} \int_{t=0}^{\infty} \frac{\mathcal{A}(t,\nu)}{t} dt, \tag{5}$$

where σ is the absorption cross section, $b \approx 3.5$ mm the probe beam diameter, and $\mathcal{A}(t,\nu) \equiv -\ln[I(t,\nu)/I_0]$ the optical density with I_0 the incident probe beam intensity. Based on the $A^2\Pi(v'=0)$ lifetime of about 20 ns,[6] we estimate that the absorption cross section is about 10^{-13} cm^2. For instance, for CaF seeded in Ar, we obtain, by integrating over the shaded area in Fig. 2(a), $\int(\mathcal{A}(t,\nu)/t)dt \approx 0.02$. As a re-

sult, $N(\nu_0) \approx 10^{11}$. Assuming a significant population of about 30 rotational states (corresponding to $T = 140$ K), we see that the total number of CaF molecules contained in a single pulse of our microbeam comes out again close to 10^{12}.

The number density formula (4) omits the effect of Mach number focusing;[8] since this decreases with the increasing mass of the carrier it is expected to be most pronounced for He, as observed. On the other hand, the best cooling/slowing is obtained in Xe, thanks to its large mass and a sizable elastic scattering cross section.

As the technique is simple and versatile, a variety of applications are likely to emerge, particularly when nonvolatile or highly reactive or unstable species need be introduced into the gas phase for collisional or spectroscopic studies.[11] The small size of the source chamber, laser induced rather than mechanical pulsing, and minimal pumping requirements are particularly advantageous. As noted, these features even make it feasible to mount the source on a high-speed rotor. More generally, the source should be useful whenever a molecular beam needs to be generated in a region too small to attain fast pumping.

ACKNOWLEDGMENTS

The authors thank John Doyle and Jack Harris (Harvard University) for helpful discussions. This work has been supported by a grant from the U.S. Department of Energy and the Petroleum Research Fund of the American Chemical Society. One of the authors (B.S.Z.) thanks the Korean Program BK21 for a stipend, and one of the authors (M.C.), the Spanish Ministry of Culture and Education for a Fellowship.

[1] *Atomic and Molecular Beam Methods*, edited by G. Scoles (Oxford University Press, Oxford, U.K., 1988), Vol. I.
[2] *Atomic and Molecular Beams: The State of the Art 2000*, edited by R. Campargue (Springer, Berlin, 2001).
[3] W. Gentry, in *Atomic and Molecular Beam Methods*, edited by G. Scoles (Oxford University Press, Oxford, U.K., 1988), Vol. I.
[4] R. E. Smalley, Rev. Mod. Phys. **69**, 723 (1997).
[5] M. Gupta and D. Herschbach, J. Phys. Chem. A **103**, 10670 (1999); **105**, 1626 (2001).
[6] S. N. Suchard, *Heteronuclear Diatomic Molecules* (Plenum, New York, 1975), Vol. I, p. 389.
[7] J. D. Weinstein, R. deCarvalho, T. Guillet, B. Friedrich, and J. M. Doyle, Nature (London) **395**, 148 (1998).
[8] S. DePaul, D. Pullman, and B. Friedrich, J. Phys. Chem. **97**, 2167 (1993).
[9] R. W. Field, D. O. Harris, and T. Tanaka, J. Mol. Spectrosc. **57**, 107 (1975).
[10] R. deCarvalho, J. M. Doyle, B. Friedrich, T. Guillet, J. Kim, D. Patterson, and J. Weinstein, Eur. Phys. J. D **7**, 289 (1999).
[11] J. C. Polanyi, in *Atomic and Molecular Beams: The State of the Art 2000*, edited by R. Campargue (Springer, Berlin, 2001).